# Methods for Identification of Feedback Control During Standing

Samin Askarian, Antonie J. van den Bogert*

*Department of Mechanical Engineering, Cleveland State University*
*Cleveland, OH 44115, USA*

**Abstract**

The mechanism of human balance control could be studied by a direct approach (DA) in which a relationship between observed joint moments and potential feedback signals was identified. However, the human balance system operates in a closed loop and this would bias the estimated controller towards the inverse of the plant, i.e. inverse multibody dynamics. The aim of this paper was to validate the direct approach method for identification of feedback control in human standing and to study the effect of platform perturbation amplitude on the accuracy of the DA identification technique. Furthermore, indirect approach (IA) was used for the same system to remove the systematic error in gain estimation. Test data were obtained from a simulation in which the plant was modeled as a double inverted pendulum, perturbed with horizontal accelerations at the base to mimic a test protocol for human standing balance. Controller gains were estimated according to the DA by a linear least squares method to fit a proportional derivative (PD) controller model to the data. As expected, systematic errors were found in the estimated controller gains but these systematic errors decreased with increasing amplitudes of external perturbation. It was concluded that the DA can estimate feedback gains for human postural control, when sufficiently large external perturbations are applied. To apply the IA, the appropriate cost function was considered and no constraint was applied on optimization process, instead some criteria were defined to stop the simulation process before the system gets into unstable region. It was shown that IA didn't have the limitation of generating systematic error even for small perturbations.

*Keywords:* control identification, direct approach, indirect approach, double link inverted pendulum, perturbations.

*Corresponding author
*Email address:* a.vandenbogert@csuohio.edu ( Antonie J. van den Bogert)

## 1. Introduction

The keen interest in identification of feedback control gains in human balance system with the aim of replicating the real motion has resulted in a vast area of research. It has been shown that postural sway can be modeled as an inverted pendulum and it has been verified experimentally [23, 3, 9]. In the context of quiet standing early works were based on modeling a human dynamics with single inverted pendulum[18, 15] whereas recently it has been proven that multi segment models should be used to model sway motion to get accurate results [19, 5]. Generally, balance control studies can be divided into two categories of perturbed and unperturbed/quiet standing and different measurements of joint moments, angles, angular velocities, center of mass(COM) and center of pressure(COP) are used to identify the feedback controller gains used in human balance control. Identification technique used in closed systems are categorized into three different methods [14]: direct approach, indirect approach and joint input-output method. In some works [4, 23] direct approach was used and cross-correlation analysis was applied to identify the time shift between COP and COM. Masani et al.[16] applied linear regression of ankle torque and ankle angle to estimate the feedback gain, it was also shown that to eliminate the delay in closed loop system it's not necessary to apply feed-forward mechanism in quiet standing and promotional derivative (PD) controller is a good approximation for control strategy.

It was well accepted that direct approach is a valid method for open loop systems [10, 14, 21] in which the input and associated output signal reflects the dynamics of the plant whereas in the closed loop system the relation between input and output inherits the information about both plant and controller.

Johansson et.al [7] applied indirect approach to identify feedback gains used in maintaining postural control. In this study the model made compatible with spectra analysis and parametric estimation was performed. Later on the indirect approach was used to provide the linear dynamic response models which was suitable to fit the individual test subjects and had the capability of predicting the motion during perturbed but stable stance accurately [8]. Park et.al [17] also used indirect approach to estimate feedback gains for perturbed standing, the equations of motion for double link inverted pendulum were linearized around the upright position and feedback gains were estimated for different perturbation magnitudes. The Constrained optimization was used to perform the gain estimation. The constrain was placed on optimization to make the closed loop system stable. It was shown in this work that trajectories of joint angles and torques were related to amount of perturbation and they were scaled gradually [11]. Kuo [13, 12] used stochastic model with noise as disturbance to body and errors in sensors, studied sensitivity of postural behavior to variations in amount of these parameters. It was concluded that central nervous system (CNS) had chosen feedback control being aware of system dynamics and the model could predict the postural response under altered sensory conditions [2].

The purpose of the present study was to apply direct and indirect identification method to estimate the feedback gains in human balance control system. The effect of perturbation magnitude modeled with Brownian motion was investigated on biased introduced using direct approach and it was shown to what extent multi-joint human feedback control can be estimated using direct approach. Furthermore, indirect approach was applied to the same nonlinear plant dynamics system to remove biased from gain estimation for small perturbations. In this method, no constraint was used during optimization process, instead some criteria were defined to stop the simulation before the system gets unstable.

## 2. Simulation Model

In this section the simple model of human balance control will be introduced (Fig. 1) and this model will be used to generate the estimated joint angles, angular velocities and associated torques. In section 2.2 the dynamics of the double link inverted pendulum(DIP)and controller properties are described and the equations of motions are presented. In section 2.3 the solution of closed loop system is derived and the realistic motion is simulated.

### *2.1. Simple model of human balance control*

Human balance control system is a closed loop feedback system (Fig. 1). The plant in this system, representing body dynamics is modeled as the DIP system on a platform. The platform can move horizontally and have an acceleration of $W$. The effect of gravity and acceleration of the platform can make the system unstable, therefore a feedback control system is used to counteract these effects and create enough torques to balance the DIP system. The input to the body dynamics block is the generated torques and controller noise ($v$), and the output is system state. This simplified human balance control system is used to estimate the the amount of torques, angles and angular velocities at body joints.

### *2.2. Plant dynamics and controller*

Many previous works had shown that body sway during quiet standing can be modeled by inverted pendulum [23]. The DIP system used in this work has two joints at ankle and hip and two controlling torques were applied at these joints (Fig. 2). The first link represented the leg and the second link was extended from hip to the shoulder. It is assumed that change in knee angle is negligible. The angles $\theta_1$ and $\theta_2$, were measured

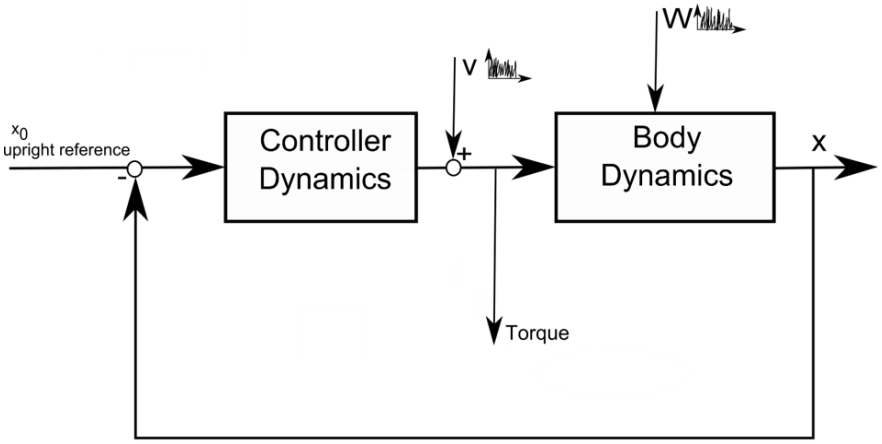


Figure 1: Simple model of human balance control system

with respect to vertical position and they were zero at the balance position. $m_1$ and $m_2$ denotes masses of first and second link respectively; $l_1$ and $l_2$ are the distance between the pivot and the center of mass of each link; $L_1$ and $L_2$ are the length of first and second link respectively. It was assumed there is no friction in the system and the masses are distributed homogeneously. The Euler-Lagrange method was used to derive the equations of motion for DIP system. This method is based on determining the kinetic and potential energy of the system in terms of the generalized coordinates. Equation (1) is the equations of motion for DIP system and $W$ is the acceleration of the platform as shown in Fig. 2. The derivation of equations of motion for DIP system is presented in Appendix A and the equations of motions are converted to the state space form by implementing the following change of variables: $x_1 = \theta_1$,$x_2 = \dot{\theta}_1$, $x_3 = \theta_2$ and $x_4 = \dot{\theta}_2$.

$$
\begin{aligned}
h_1 cos\theta_1 W + h_3 \ddot{\theta_1} + h_4 cos(\theta_1 - \theta_2)\ddot{\theta_2} - h_6 sin\theta_1 + h_4 \dot{\theta_2}^2 sin(\theta_1 - \theta_2) - T_1 = 0 \\
h_2 cos\theta_2 W + h_5 \ddot{\theta_2} + h_4 cos(\theta_1 - \theta_2)\ddot{\theta_1} - h_7 sin\theta_2 - h_4 \dot{\theta_1}^2 sin(\theta_1 - \theta_2) - T_2 = 0
\end{aligned} \tag{1}
$$

The controller used in human balance control system was proportional derivative (PD) type it was a $2 \times 4$ matrix, each gain in feedback matrix specified the amount of torque generated in each joint for change in angle and angular velocities of that joint.

### *2.3. Simulation*

The test data was generated by DIP simulation of human balance control. The closed loop equations were derived by applying the feedback law given in Eq.(2) , where $X$ is the system state, K is the controller matrix

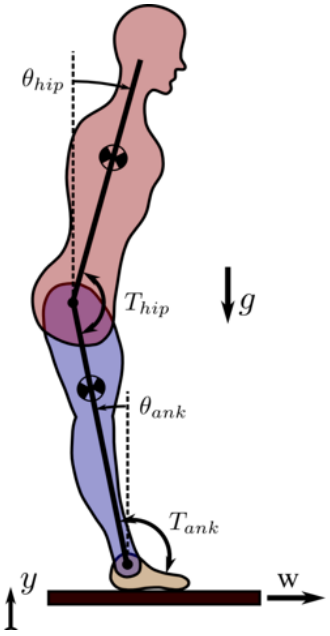


Figure 2: Biomechanical posture model in sagittal plane

and T is joint torques.

$$T = -\mathbf{K}X \tag{2}$$

$$\begin{bmatrix} T_1 \\ T_2 \end{bmatrix} = - \begin{bmatrix} K_{11} & K_{12} & K_{13} & K_{14} \\ K_{21} & K_{22} & K_{23} & K_{24} \end{bmatrix} \begin{bmatrix} x_1 \\ x_2 \\ x_3 \\ x_4 \end{bmatrix} \tag{3}$$

The gains used in the simulation are typical human feedback gains [17]. Dimensions and mass properties used in equations of motion were based on human with 85 kg body mass and 175 cm height. The properties used in simulating the DIP system is presented in Appendix C. The platform acceleration ($W$) and controller noise ($v$) were modeled by Brownian motion. The reason for choosing a Brownian motion to model the platform acceleration is to replicate the data generated from experiment in human motion and control lab. The presence of Brownian motion in the differential equations of closed system, had resulted in a set of stochastic differential equations. The approximate numerical solution to the stochastic systems of equations were achieved using Euler-Maruyama method [6] which is the generalization of Euler method for ordinary

differential equations to stochastic differential equations. Details of Euler-Maruyama method is explained in Appendix B. Therefore, the closed loop system equations in martix form has the following format:

$$\begin{bmatrix} T_1 \\ T_2 \end{bmatrix} = - \begin{bmatrix} K_{11} & K_{12} & K_{13} & K_{14} \\ K_{21} & K_{22} & K_{23} & K_{24} \end{bmatrix} \begin{bmatrix} x_1 \\ x_2 \\ x_3 \\ x_4 \end{bmatrix} + \begin{bmatrix} dW_2 \\ dW_3 \end{bmatrix} \tag{4}$$

The discritized equations of motion using Euler-Maruyama method in matrix format is (Eq.(5))

$$X_j = X_{j-1} + \left( \mathbf{W}(X_{j-1}) dW_1(j-1) + \mathbf{A}(X_{j-1}) + \mathbf{B}(X_{j-1}) \begin{bmatrix} T_1 \\ T_2 \end{bmatrix} \right) \Delta t \tag{5}$$

Where $dW_1$, $dW_2$ and $dW_3$ are Brownian increments representing platform acceleration, controller noise on ankle torque and hip torque consequently. Matrices $\mathbf{W}$,$\mathbf{A}$ and $\mathbf{B}$ are depending on state of system $X = \begin{bmatrix} x_1 & x_2 & x_3 & x_4 \end{bmatrix}^T$ and they get updated at each point of time. The expressions for these matrices are presented in Appendix B. It should be mentioned that in this case the Brownian increments are defined as random variable of the form $dW1 = N(0, \sigma_w)/\sqrt{\Delta t}$ ,$dW2 = N(0, \sigma_v)/\sqrt{\Delta t}$ and $dW2 = N(0, \sigma_v)/\sqrt{\Delta t}$ where $\sigma_w$ and $\sigma_v$ are standard deviation of platform acceleration and controller noise. The magnitude of $\sigma_w$ was chosen to produce realistic perturbation response [17] when the controller noise is zero. Furthermore, magnitude of $\sigma_v$ was selected to model the realistic sway during quiet standing (when $dW1 = 0$) [1]. Based on the system properties platform perturbation ($\sigma_w$) could change from 0 to 0.4 $ms^{-2}\sqrt{Hz}$ and controller noise variance was selected to be $\sigma_v = 0.5 \quad ms^{-2}\sqrt{Hz}$. The closed loop systems of stochastic differential equations were solved to simulate the motion for 100 seconds. The time step used for modeling was 0.1 mili-seconds and simulation was done over 500 different Brownian paths. Estimated torques and system state (angles and angular velocities of the joints) were sampled at 100 Hz. This data was used for direct approach identification technique.

## 3. Direct Approach

Direct approach identification technique can be used in closed loop systems to identify the controller based on input(estimated angles and angular velocities) and output (estimated torque) data of the controller . The

advantage of this method is that it doesn't require the plant information. van der Kooij et. al [21] had shown that direct approach can result in erroneous identification in a closed loop system with a frequency domain methods. The purpose of this work is to study the effect of amount of platform perturbation ($W$) and controller noise on identifying the feedback gains using direct approach.

To estimate the feedback gains, linear least square estimation was used method to fit a PD controller model to the data. The feedback gain matrix $\mathbf{K}$ was unknown, $T$ and $X$ matrices have the same number of columns which were the total numeber of time steps. Therefore, gains were estimated (using matrix right hand side division)for each of the Brownian paths; mean and standard deviation of each gain was obtained over 500 Brownian paths. This procedure was repeated for different platform accelerations.

## 4. Indirect Approach

To study the control strategy that human body used to balance itself in response to small perturbation, another technique was applied. In this method indirect approach was used to explain the selection of control strategies [12]. This identification technique was based on using optimization to select feedback gains such that the human balance model would reproduce experimental response in each trial. In this work, instead of experimental data, we used data generated in section 2.3. To avoid confusion, this data would be referred as base data and only one of the Brownian paths had been selected for this modeling. The goal was to identify 8 feedback controller gains such that human balance system would reproduce the same trajectory as the based data. The cost function would be to minimize the sum-squared, normalized deviation of the model state ($\mathbf{x}_{sim}$)and torques ($\mathbf{T}_{sim}$) from the based data ($\mathbf{x}_b$ and $\mathbf{T}_b$) [17]. Furthermore, the effect of duration of simulation ($t_{end}$) was taken into consideration by adding the term $r/tend$ to a cost function where $r$ is a constant and was chosen to be 10,000 to have equivalent weight as the first term of objective function. The goal was to minimize the cost function by finding the appropriate controller gains that could replicate the 100 seconds of simulation. The cost function was defined as:

$$f(\mathbf{K}) = \sum_{i=1}^{L_s}(\frac{\mathbf{x}_{sim} - \mathbf{x}_b}{max(\mathbf{x}_b)})^2 + \sum_{i=1}^{L_s}(\frac{\mathbf{T}_{sim} - \mathbf{T}_b}{max(\mathbf{T}_b)})^2 + \frac{r}{t_{end}} \tag{6}$$

In Eq.(6), $\mathbf{x}_{sim}$ is a $4 \times L_s$ matrix and $\mathbf{T}_{sim}$ is a $2 \times L_s$ matrix and the summation is over sampled data. During the optimization process, initial guess would be selected for 8 feedback gains and the simulation

data would be obtained by solving closed loop systems of equations.It should be mentioned that controller noise was zero in simulation. There was a chance that guessed feedback gains made the system unstable, therefore, four criteria were defined to stop the simulation and simulation duration $t_{end}$ was determined using interpolation and used in cost function. The four criteria were defined as follow:

1. If $|\theta_1| > \pi/2$ simulation would be terminated and $t_{end}$ determined.
2. If $|\theta_2| > \pi/2$ simulation would be terminated and $t_{end}$ determined.
3. If cost function was larger than a critical value,$f > f_c$, simulation was terminated and $t_{end}$ determined.
4. If none of the above conditions ocurred $t_{end} = 100s$ which means that simulation was performed for the total duration.

In this work, MATLAB optimization toolbox was used and fmincon function with "interior-point" algorithm was selected. It should be mentioned that no constraint were used in this method, instead those four criteria were applied in conjunction with modification of cost function to account for being in stable region during simulation. for each case study the simulation was done over 20 Brownian paths, mean and standard deviations were obtained for feedback gains.

## 5. Results and Discussion

### *5.1. Direct approach*

Data was generated for a perturbation with standard deviation ($\sigma_w$) ranging from 0 to 0.4 $ms^{-2}\sqrt{Hz}$ with 0.001 step size. The estimated feedback gains were obtained for each perturation and it was averaged over 100 Brownian paths. In Fig.3, the average value of feedback gains were presented with the true value of gains used in generating the data and Error bars showed the 95 percent confidence interval at each perturbation magnitude. For quiet standing ($\sigma_w$=0), the controller gain estimates were biased towards values that represent the inverse of the plant dynamics. For instance, the feedback gains from ankle angle to ankle moment ($K_{11}$) was overestimated. This is consistent with the van der Kooij [21] findings on a single link system using frequency domain method. As the perturbation magnitude increased, the biased decreased along with the random error (Fig.3).

The largest perturbation magnitude that was tested, generated joint rotations of maximum 12 degree which are not excessive for human experiment. The results showed that reproducible and unbiased identification of human feedback control should be possible when perturbations were large enough. Further work could be done on the same system to do sensitivity analysis.

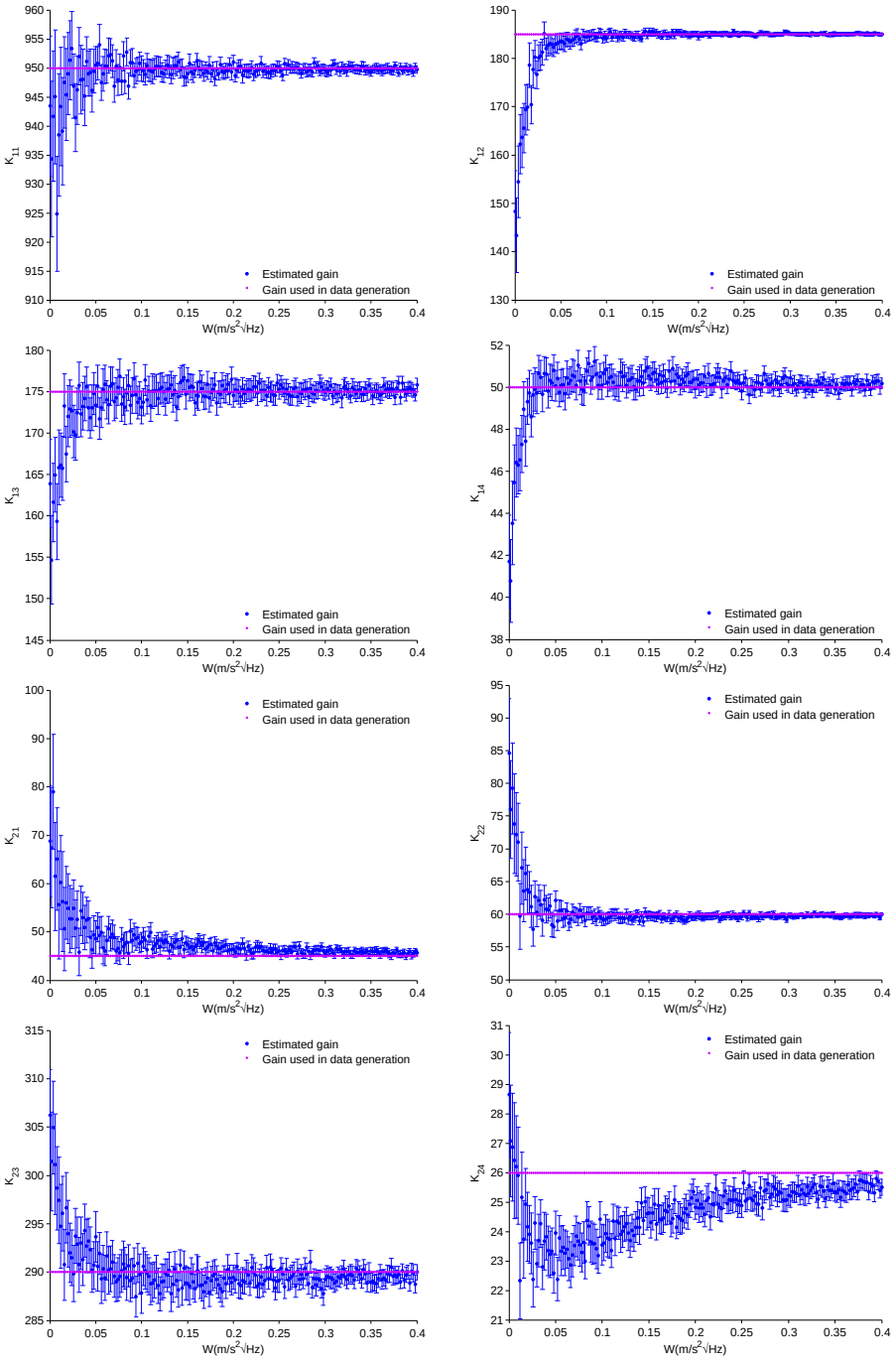


Figure 3: Estimated feedback gains using direct approach $Mean \pm SE(N = 500)$

*5.2. Indirect Approach*

Since the system of equations are nonlinear, initial guess would effect the convergence of optimization process. To investigate dependency of convergence on initial guess, simulation was performed for ten random initial guesses and seven simulations could converge to the true feedback gains used in data generation.

To study the effect of velocity and torques in the cost function, three sets of simulation were performed. In the first simulation cost function included system state (angles and angular velocities) and joint torques. The simulation was performed for 20 different Brownian paths and platform perturbation was set to its largest value, $\sigma_w = 0.4 \quad (ms^{-2}\sqrt{Hz})$. In the second simulation angular velocities were excluded from cost function and for the third simulation both angular velocities and torques were excluded. To make the comparison possible, the same 20 data sets were used for these three types of estimation. The mean value of estimated feedback controller gains (over 20 data sets) was used to generate the motion and the result was compared with one of the data sets (In which the motion was simulated with a true feedback gains) and the root mean square (rms) of the difference between these two data was obtained. The results are presented in Table.1 for these three studies. The results indicated that by excluding both velocities and torques from the cost function, the accuracy of estimation would decrease, therefore rms values increased. Another way to show the effect of excluding torques and velocities from the cost function is comparing the feedback gains' mean and standard deviation values for these three cases. The results were presented in Table.2. These results were consistent with outcome of rms values, excluding both torques and velocities would increase the standard error and deviation of mean value from its true one.

Table 1: Comparing RMS for different format of cost function $\sigma_w = 0.4$

| | Root Mean Square | | |
|---|---|---|---|
| | exclude velocities | exclude torques | exclude both |
| $\Theta_1$ | 0.0002 | 0.0002 | 0.0003 |
| $\dot{\Theta}_1$ | 0.0004 | 0.0006 | 0.0009 |
| $\Theta_2$ | 0.0003 | 0.0003 | 0.0004 |
| $\dot{\Theta}_2$ | 0.0008 | 0.0008 | 0.0010 |
| $\mathbf{T}_1$ | 0.2569 | 0.3500 | 0.4948 |
| $\mathbf{T}_2$ | 0.1102 | 0.1229 | 0.1672 |

To compare the direct and indirect identification technique for small platform perturbation, the following study was done. For this purpose, $\sigma_w = 0.01 \quad (ms^{-2}\sqrt{Hz})$ was selected for which biased was noticeable in the direct approach identification. The indirect technique was used and the simulation was done for 20 different data sets, mean and standard deviation of $\mathbf{K}$ matrix was evaluated over these paths. The standard

Table 2: Gain estimation for different format of cost functions $\sigma_w = 0.4$

| | $Mean \pm SD(N = 20)$ | | | |
|---|---|---|---|---|
| | exclude velocities | exclude torques | exclude both | True Value |
| $K_{11}$ | $953.21 \pm 8.41$ | $954.72 \pm 10.91$ | $956.78 \pm 12.56$ | 950 |
| $K_{12}$ | $183.62 \pm 3.31$ | $182.72 \pm 4.74$ | $181.92 \pm 5.50$ | 185 |
| $K_{13}$ | $169.23 \pm 14.08$ | $165.27 \pm 19.68$ | $162.68 \pm 22.85$ | 175 |
| $K_{14}$ | $48.63 \pm 5.77$ | $47.48 \pm 7.61$ | $46.68 \pm 8.54$ | 50 |
| $K_{21}$ | $46.11 \pm 2.95$ | $46.82 \pm 3.94$ | $47.32 \pm 4.56$ | 45 |
| $K_{22}$ | $59.32 \pm 1.29$ | $59.06 \pm 1.74$ | $58.77 \pm 2.01$ | 60 |
| $K_{23}$ | $287.46 \pm 4.96$ | $286.14 \pm 6.84$ | $285.14 \pm 7.92$ | 290 |
| $K_{24}$ | $34.40 \pm 2.10$ | $33.88 \pm 2.68$ | $33.66 \pm 2.99$ | 35 |

error of feedback gains in direct approach is larger than indirect method (Table.3). These results showed that indirect method could be used even for small perturbations and the biased would be removed. The direct approach had the advantage of being easier to apply and it didn't require the plant information, however, it leads to erroneous results for small platform perturbations. The indirect approach had the disadvantage of requiring plant information but it could estimate the gains for small perturbations. This outcome is consistent with the results of Kooij et.al work[21].

Table 3: $Mean \pm SD$ for $\sigma_w = 0.01$ using direct and indirect approach

| | $Mean \pm SD$ | | |
|---|---|---|---|
| | $IA(N = 20)$ | True Value | $DA(N = 500)$ |
| $K_{11}$ | $951.21 \pm 1.57$ | 950 | $938.44 \pm 12.22$ |
| $K_{12}$ | $183.23 \pm 2.00$ | 185 | $165.54 \pm 5.96$ |
| $K_{13}$ | $172.16 \pm 3.14$ | 175 | $165.82 \pm 5.23$ |
| $K_{14}$ | $50.20 \pm 1.16$ | 50 | $46.31 \pm 16.04$ |
| $K_{21}$ | $45.43 \pm 2.66$ | 45 | $55.62 \pm 12.92$ |
| $K_{22}$ | $61.74 \pm 4.46$ | 60 | $71.03 \pm 6.85$ |
| $K_{23}$ | $289.10 \pm 2.68$ | 290 | $297.41 \pm 5.18$ |
| $K_{24}$ | $25.52 \pm 1.16$ | 26 | $25.89 \pm 1.93$ |

## 6. Conclusion

In this paper the human balance control system was modeled by a simple feedback closed loop system and the plant was DIP system, this model was used to generate the motion data and two different identification approach was applied to estimate the feedback gains. Since the human balance system operated in a closed loop and this would bias the estimated controller towards the inverse of the plant dynamics. This bias depended on the amount of controller noise and the amount of external perturbation applied to the system. It was shown that direct approach could be used to estimate the feedback gains when perturbations are large enough and the systematic errors were large for small platform perturbations. However, the indirect approach didn't have this limitation and biased was removed for small perturbations. It was also shown that the velocities and torques measurements could be removed from cost function without altering the estimation significantly. Since torque and velocity measurements are usually noisy, not including them in the cost function would help. The effect of noise on data hasn't been considered in this work and in future studies the model can be modified to represent the more realistic situation.

**Appendix A**

The equations of motion for double link inverted pendulum is obtained using the Euler-Lagrange method. Equation (A-1) denotes the form of Lagrangian equation used in this work where $L = T - V$. Kinetic and potential energy of the system are represented by $T$ and $V$ respectively. The generalized coordinate is $q$ and $Q_q$ is the generalized torque. For DIP system the generalized coordinates are $\theta_1$ and $\theta_2$. The system kinetic energy is:

$$\frac{d}{dt}(\frac{\partial L}{\partial \dot{q}}) - \frac{\partial L}{\partial q} = Q_q \tag{A-1}$$

$$T = T_{pendulum1} + T_{pendulum2} \tag{A-2}$$

where

$$\begin{aligned} T_{pendulum1} &= \frac{1}{2} m_1[(\dot{x} + l_1\dot{\theta_1} cos\theta_1)^2 + (l_1\dot{\theta_1} sin\theta_1)^2] + \frac{1}{2} J_1 \dot{\theta_1}^2 \\ T_{pendulum2} &= \frac{1}{2} m_2[(\dot{x} + L_1\dot{\theta_1} cos\theta_1 + l_2\dot{\theta_2} cos\theta_2)^2 + (L_1\dot{\theta_1} sin\theta_1 + l_2\dot{\theta_2} sin\theta_2)^2] + \frac{1}{2} J_2 \dot{\theta_2}^2 \end{aligned} \tag{A-3}$$

$J_1$ and $J_2$ are the moment of inertia with respect to the center of gravity for the first and second link respectively. The location of a platform is presented by $x$. The potential energy of the system $V$ is:

$$V = V_{pendulum1} + V_{pendulum2} \tag{A-4}$$

$$V = m_1 g l_1 cos\theta_1 + m_2 g(L_1 cos\theta_1 + l_2 cos\theta_2) \tag{A-5}$$

Therefore, the Euler-Lagrange equations of the DIP system in compact notation are:

$$\begin{aligned} h_1 cos\theta_1 \ddot{x} + h_3 \ddot{\theta_1} + h_4 cos(\theta_1 - \theta_2)\ddot{\theta_2} - h_6 sin\theta_1 + h_4 \dot{\theta_2}^2 sin(\theta_1 - \theta_2) - T_1 = 0 \\ h_2 cos\theta_2 \ddot{x} + h_5 \ddot{\theta_2} + h_4 cos(\theta_1 - \theta_2)\ddot{\theta_1} - h_7 sin\theta_2 - h_4 \dot{\theta_1}^2 sin(\theta_1 - \theta_2) - T_2 = 0 \end{aligned} \tag{A-6}$$

where the constants are defined as follow:

$$
\begin{aligned}
h_1 &= m_1 l_1 + m_2 L_1 \\
h_2 &= m_2 l_2 \\
h_3 &= m_1 l_1^2 + m_2 L_1^2 + J_1 \\
h_4 &= m_2 l_2 L_1 \\
h_5 &= m_2 l_2^2 + J_2 \\
h_6 &= m_1 l_1 g + m_2 L_1 g \\
h_7 &= m_2 l_2 g
\end{aligned}
\tag{A-7}
$$

As the next step the equations of motions are converted to the state space form by implementing the following change of variables: $x_1 = \theta_1$,$x_2 = \dot{\theta}_1$, $x_3 = \theta_2$ and $x_4 = \dot{\theta}_2$.

$$
\begin{aligned}
&\dot{x_1} = x_2 \\
&\dot{x_3} = x_4 \\
&h_1 cos\theta_1 \ddot{x} + h_3 \dot{x_2} + h_4 cos(x_1 - x_3)\dot{x_4} - h_6 sin x_1 + h_4 x_4^2 sin(x_1 - x_3) - T_1 = 0 \\
&h_2 cos x_3 \ddot{x} + h_5 \dot{x_4} + h_4 cos(x_1 - x_3)\dot{x_2} - h_7 sin x_3 - h_4 {x_2}^2 sin(x_1 - x_3) - T_2 = 0
\end{aligned}
\tag{A-8}
$$

**Appendix B**

The first order stochastic differential equation can be described by Eq.(B-1), where $w(t)$ is the mean zero Gaussian white noise.

$$\frac{dX(t)}{dt} = f(X(t),t) + g(X(t),t)w(t) \tag{B-1}$$

Integrating Eq.(B-1) from initial time ,$t_0$, to time $t$ results in:

$$X(t) - X(t_0) = \int_{t_0}^{t} f(X(s),s)\,ds + \int_{t_0}^{t} g(X(s),s)w(s)\,ds \tag{B-2}$$

where $w(t)dt$ is the increment of another process called Brownian motion [20].

$$\int_{t_0}^{t} g(X(s),s)w(s)\,ds = \int_{t_0}^{t} g(X(s),s)\,dW(s) \tag{B-3}$$

Therefore, the stochastic differential equation reduced to the form in Eq.(B-4).

$$X(t) - X(t_0) = \int_{t_0}^{t} f(X(s),s)\,ds + \int_{t_0}^{t} g(X(s),s)\,dW(s) \tag{B-4}$$

For computational purposes the discretized Brownian motion is specified as $W_j$ which denotes $W(t_j)$ with $t_j = j\delta t$ where $\delta t = t_f/N$. $t_f$ is the simulation duration and N is a positive integer. According to three defined conditions for Brownian motion process:

$$W_j = W_{j-1} + dW_j, \qquad j = 1, 2, \cdots, N \tag{B-5}$$

where each $dW_j$ is an independent random variable of the form $\sqrt{\delta t}N(0,1)$.
To discretize Eq.(B-4) over time interval $[0, t_f]$ the time step $\Delta t = t_f/L$ is considered for some positive integer $L$, and $\tau_j = j\Delta t$. The numerical approximation to $X(\tau_j$ is denoted by $X_j$. Therefore, the Euler-Maruyama method takes the form (Eq.(B-6)).

$$X_j = X_{j-1} + f(X_{j-1})\Delta t + g(X_{j-1})(W(\tau_j) - W(\tau_{j-1})) \tag{B-6}$$

It is easier to choose the step size $\Delta t$ for numerical method to be an integer multiple of the increment $\delta t$ for the Brownian path. In this way the discretized Brownian path contains the points $\tau_j$ at which Euler-Maruyama solution is computed. In this work, the same tim step was chosen for discretizing Brownian path and the numerical method. The discritized DIP equations of motion using Euler-Maruyama method in matrix format is (Eq.(B-7))

$$X_j = X_{j-1} + (\mathbf{W}(X_{j-1})dW_1(j-1) + \mathbf{A}(X_{j-1}) + \mathbf{B}(X_{j-1}) \begin{bmatrix} T_1 \\ T_2 \end{bmatrix})\Delta t \tag{B-7}$$

Where $dW_1$, $dW_2$ and $dW_3$ are Brownian increments representing platform accelaration, controller noise on ankle torque and hip torque consequently. Matrices $\mathbf{W}$,$\mathbf{A}$ and $\mathbf{B}$ are as follow:

$$\mathbf{W} = \begin{bmatrix} 0 \\ \frac{-a_3 cos x_1 + a_4 cos x_3 cos(x_1 - x_3)}{a_1 - a_2 cos^2(x_1 - x_3)} \\ 0 \\ \frac{-a_9 cos x_3 + a_8 cos x_1 cos(x_1 - x_3)}{a_1 - a_2 cos^2(x_1 - x_3)} \end{bmatrix}$$

$$\mathbf{A} = \begin{bmatrix} x_2 \\ \frac{(-a_5 x_4^2 - a_2 x_2^2 cos(x_1 - x_3))sin(x_1 - x_3) + a_6 sin x_1 - a_7 sin x_3 cos(x_1 - x_3)}{a_1 - a_2 cos^2(x_1 - x_3)} \\ x_4 \\ \frac{(b_1 x_2^2 + a_2 x_4^2 cos(x_1 - x_3))sin(x_1 - x_3) + b_3 sin x_3 - b_2 sin x_1 cos(x_1 - x_3)}{a_1 - a_2 cos^2(x_1 - x_3)} \end{bmatrix}$$

$$\mathbf{B} = \begin{bmatrix} 0 & 0 \\ \frac{h_6}{a_1 - a_2 cos^2(x_1 - x_3)} & \frac{-h_5 cos(x_1 - x_3)}{a_1 - a_2 cos^2(x_1 - x_3)} \\ 0 & 0 \\ \frac{-h_5 cos(x_1 - x_3)}{a_1 - a_2 cos^2(x_1 - x_3)} & \frac{h_4}{a_1 - a_2 cos^2(x_1 - x_3)} \end{bmatrix} \tag{B-8}$$

where $a_1, a_2, a_3, a_4, a_5, a_6, a_7, a_8, a_9, b_1, b_2$ and $b_3$ are constants and defined based on parameters given in Appendix A.

$$\begin{array}{lll} a_1 = h_5 h_3 & a_2 = h_4^2 & a_3 = h_5 h_1 \\ a_4 = h_4 h_2 & a_5 = h_5 h_4 & a_6 = h_5 h_6 \\ a_7 = h_4 h_7 & a_8 = h_4 h_1 & a_9 = h_3 h_2 \\ b_1 = h_3 h_4 & b_2 = h_4 h_6 & b_3 = h_3 h_7 \end{array} \tag{B-9}$$

## Appendix C

Dimensions and mass properties of DIP model that were based on [22] and presented in Table 5. The first link and second link are referred to with indices 1 and 2 respectively. mass of the link is indicated with $m$, $L$ is total length of the link and $L_c$ is the distance between the joint and center of mass of the same link, $J$ is the moment of inertia with respect to the center of mass. The total body mass of the human considered to be $M = 85 \quad kg$ and height of $H = 1.75 \quad m$.

Table 4: Average anthropometric data

| Dimensions and mass properties of links | |
|---|---|
| $m_1$ | $0.322M$ |
| $m_2$ | $0.678M$ |
| $L_1$ | $0.53H$ |
| $L_2$ | $0.288H$ |
| $L_{c1}$ | $0.523L_1$ |
| $L_{c2}$ | $0.626L_2$ |
| $J_1$ | $m(0.326L_1)^2$ |
| $J_2$ | $m(0.496L_2)^2$ |

The typical controller gains selected for this work is presented in Eq.(C-1).

$$\mathbf{K} = \begin{bmatrix} 950 & 185 & 175 & 50 \\ 45 & 60 & 290 & 26 \end{bmatrix} \tag{C-1}$$

## References


[1] Briac Colobert, Armel Crtual, Paul Allard, and Paul Delamarche, *Force-plate based computation of ankle and hip strategies from double-inverted pendulum model*, Clinical Biomechanics **21** (2006), no. 4, 427 – 434.

[2] N. Fujisawa, T. Masuda, H. Inaoka, Y. Fukuoka, A. Ishida, and H. Minamitani, *Human standing posture control system depending on adopted strategies*, Medical and Biological Engineering and Computing **43** (2005), no. 1, 107–114 (English).

[3] William H. Gage, David A. Winter, James S. Frank, and Allan L. Adkin, *Kinematic and kinetic validity of the inverted pendulum model in quiet standing*, Gait & Posture **19** (2004), no. 2, 124 – 132.

[4] Plamen Gatev, Sherry Thomas, Thomas Kepple, and Mark Hallett, *Feedforward ankle strategy of balance during quiet stance in adults*, The Journal of Physiology **514** (1999), no. 3, 915–928.

[5] Michael Gnther, Sten Grimmer, Tobias Siebert, and Reinhard Blickhan, *All leg joints contribute to quiet human stance: A mechanical analysis*, Journal of Biomechanics **42** (2009), no. 16, 2739–2746.

[6] D. Higham., *An algorithmic introduction to numerical simulation of stochastic differential equations*, SIAM Review **43** (2001), no. 3, 525–546.

[7] R. Johansson, M. Magnusson, and M. Akesson, *Identification of human postural dynamics*, Biomedical Engineering, IEEE Transactions on **35** (1988), no. 10, 858–869.

[8] Rolf Johansson, Mns Magnusson, Per A. Fransson, and Mikael Karlberg, *Multi-stimulus multi-response posturography*, Mathematical Biosciences **174** (2001), no. 1, 41 – 59.

[9] Annica Karlssonemail and Gunilla Frykberg, *Correlations between force plate measures for assessment of balance*, Clinical Biomechanics **15** (2000), no. 5, 365369.

[10] RE Kearney and IW Hunter, *System identification of human joint dynamics*, Critical Reviews in Biomedical Engineering **18** (1990), no. 1, 55–87.

[11] Seyoung Kim, Christopher G. Atkeson, and Sukyung Park, *Perturbation-dependent selection of postural feedback gain and its scaling*, Journal of Biomechanics **45** (2012), no. 8, 1379 – 1386.

[12] A.D. Kuo, *An optimal control model for analyzing human postural balance*, Biomedical Engineering, IEEE Transactions on **42** (1995), no. 1, 87–101.

[13] Arthur D Kuo, *An optimal state estimation model of sensory integration in human postural balance*, Journal of Neural Engineering **2** (2005), no. 3, S235.

[14] Lennart. Ljung, *System identification: theory for the user*, 1999.

[15] Ian D. Loram, Constantinos N. Maganaris, and Martin Lakie, *Human postural sway results from frequent, ballistic bias impulses by soleus and gastrocnemius*, The Journal of Physiology **564** (2005), no. 1, 295–311.

[16] Kei Masani, Albert H. Vette, and Milos R. Popovic, *Controlling balance during quiet standing: Proportional and derivative controller generates preceding motor command to body sway position observed in experiments*, Gait & Posture **23** (2006), no. 2, 164 – 172.

[17] Sukyung Park, FayB. Horak, and ArthurD. Kuo, *Postural feedback responses scale with biomechanical constraints in human standing*, Experimental Brain Research **154** (2004), no. 4, 417–427 (English).

[18] R. J. Peterka, *Sensorimotor integration in human postural control*, Journal of Neurophysiology **88** (2002), no. 3, 1097–1118.

[19] Ilona J. Pinter, Roos van Swigchem, A. J. Knoek van Soest, and Leonard A. Rozendaal, *The dynamics of postural sway cannot be captured using a one-segment inverted pendulum model: A pca on segment rotations during unperturbed stance*, Journal of Neurophysiology **100** (2008), no. 6, 3197–3208.

[20] Simo. Särkkä., *Applied stochastic differential equations*, November 2012.

[21] Herman van der Kooij, Edwin van Asseldonk, and Frans C.T. van der Helm, *Comparison of different methods to identify and quantify balance control*, Journal of Neuroscience Methods **145** (2005), no. 12, 175 – 203.

[22] David A. Winter, *Biomechanics and motor control of human movement*, John Wiley and Sons, Incorporated, Hoboken, New Jersey, 2009.

[23] David A. Winter, Aftab E. Patla, Francois Prince, Milad Ishac, and Krystyna Gielo-Perczak, *Stiffness control of balance in quiet standing*, Journal of Neurophysiology **80** (1998), no. 3, 1211–1221.